JOURNAL OF MARITIME RESEARCH

Vol XXI. No. II (2024) pp 428–435

ISSN: 1697-4840, www.jmr.unican.es

Numerical study on enhancing the performance of air turbines in Oscillating Water Column wave energy converters

Mamdouh Elmallah[1,*], Mohamed Shouman[1], Mohamed Elgohary[2]

ARTICLE INFO

Article history:
Received 26 Jan 2024;
in revised from 27 Jan 2024;
accepted 19 Mar 2024.

Keywords:
Oscillating Water Column wave energy converters, SRWT, Air velocity, Power output, ANSYS.

ABSTRACT

Many studies verify that fossil fuels are the main factor responsible for climate change and other environmental issues. Studies on alternate unconventional power sources have received more serious consideration. The conversion of wave energy is among several essential types of green energy. Among the frequently utilized methods for converting wave energy is the Oscillating Water Column (OWC) device. This study investigates the efficiency optimization of OWC devices by enhancing the performance of air turbines. The study is primarily concerned with the performance of air turbines performing as power take-off in OWC systems. The OWC analytical formulas for output power and overall efficiency are illustrated in this paper. The modelling and operation of a Savonius S-type rotor-based counter-rotating vertical axis wind turbine (CRWT) is investigated in this paper using a computational simulation approach. Using the software ANSYS, modelling and numerical simulation are carried out. Better performance properties can be observed in the counter-rotating model compared to a single-rotor design. The results show that these turbine adjustments contribute to noticeable enhancement in turbine performance, which directly affects the optimization of OWC efficiency. In comparison to a single-rotor wind turbine design (SRWT), the counter-rotating design has improved properties in terms of torque, power, and their corresponding coefficients. The CRWT system generates more than twice the maximum power of an SRWT. At a speed of 9 m/s, the maximum output power of CRWT is 18 W, while the power of the individual bottom rotor at the same speed is limited to 3 W.

1. Introduction.

The combustion of petroleum-based products contributes significantly to the greenhouse gases (GHG) that blanket the Earth and trap heat from the sun. Numerous studies have found that fossil fuel oil is the primary contributor to both environmental and economic problems [1]. It is more important than ever to pursue research into alternate renewable energy sources because of rising concerns about the expense and environmental effect of petroleum fuel. Wave energy conversion is among the significant renewable energy research fields [2]. In comparison to other green energy sources including biomass, geothermal, wind, and solar, waves have the highest power density. The methodology of wave generation is derived from the force of friction exerted by the wind on the sea's surface. Figure one shows the Categories of wave energy converters [3].

The OWC device is among the commonly used methods for converting wave energy, because of its simple design. Figure two provides Schematic layout of OWC device [4].

The OWC device is built up of an empty chamber that is exposed to the ocean's depths. Due to wave action, the column of water within the chamber oscillates, compressing and decompressing the air in the chamber's upper section alternately. The primary power source for the turbine is the flow of air into and out of the chamber. The turbine acts as the most crucial part

[1]Department of Marine Engineering Technology, College of Maritime Transport & Technology, Arab Academy for Science, Technology, and Maritime Transport.

[2]Marine Engineering Department, Faculty of Engineering, Alexandria University, Egypt.

[*]Corresponding author: Mamdouh Elmallah. E-mail: Mamdouhelmallah664@gmail.com.

Figure 1: Categories of devices converting the energy of waves.

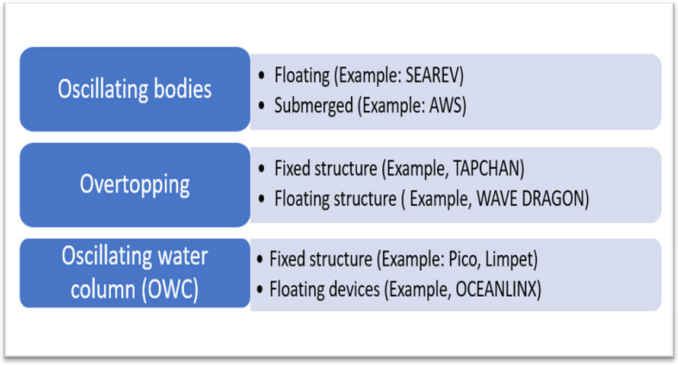

Source: Authors.

Figure 2: OWC schematic layout.

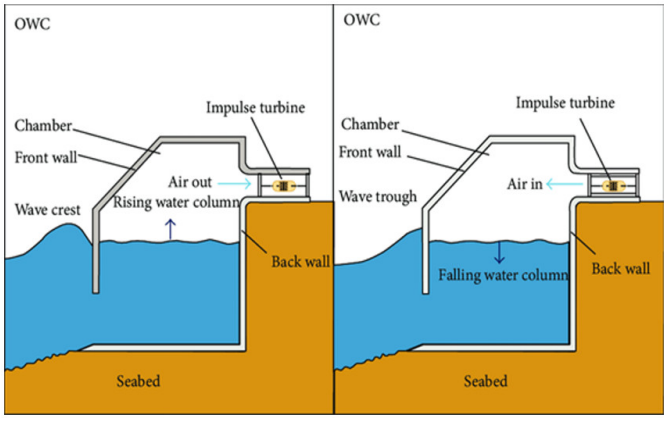

Source: Authors.

of the OWC device. Enhancing the performance of the turbine will lead to a direct optimization of the OWC system efficiency. The efficiency and output power of a OWC device are approximated in this study using a basic control volume process. Air inside the chamber serves as the control volume, and the instantaneous velocities of the inlet and outlet air are determined using the mass balance equation. The turbine's energy balance can then be used to determine the output power. [5]. The air turbine is the most significant part that affect the OWC device performance. Many studies have used the (CRWT) to enhance the performance of wind turbines. Dual rotors that operate contrary to one another form the CRWT mechanism. One of the rotors revolves anticlockwise, while the other revolves clockwise [6]. A concept like a vertical axis wind turbine (VAWT) The counter-rotating savonius wind turbine (CRSWT) principle serves as a basis for the VAWT operating principle. It has lately become accessible to VAWTs [7-11]. Additionally, numerous numerical and experimental studies have been done to analyze the flow field over Savonius wind rotors [12-22]. The basic Savonius rotor works on the theory of drag force and is made up of half-cylindrical parts attached to opposite ends of a vertical shaft. Since it cannot rotate faster than the wind speed, the tip-speed ratio must be less than or equal to 1. It functions based on the varied forces applied to each blade. The blade is driven to spin around its central vertical shaft when the concave section towards the wind direction captures the airflow. The convex portion of the blade deflects sideways and around the shaft when it collides with the air. Figure three represents the counter-rotating VAWT.

Figure 3: Counter-rotating vertical axis wind turbine.

Source: Authors.

The established formula to calculate the efficiency and output power of a OWC device is highlighted in this study. In particular, the aim of this investigation is to analyze the air turbine performance acting as power take-off in OWC systems. In this study, a CFD modelling and simulation using the ANSYS FLUENT is used to focus on the enhancing of the air turbine performance. The study simulates the turbine performance of (CRSWT). As opposed to the straight-bladed H-type rotor, the Savonius S-type rotor is well known for its inherent features that operate at lower air speeds. This rotor is therefore anticipated to improve a single-rotor VAWT system's conversion efficiency.

2. Mathematical formulas.

It is crucial to illustrate the theory and mathematical formula of the OWC device. Based on Sameti et al. (2014) [5],

The inverted cylinder and piston arrangement, shown in figure four, is a simple concept for capturing energy from the up-and-down action of the waves. The wave action causes the buoyant piston to move vertically. Because the ocean sinusoidal wave's shape is different from the water surface in the chamber, one piston model that can be used is the deformable sinusoidal piston. Any losses are ignored in order to acquire the highest available power. An additional assumption for the study is that the chamber's air is incompressible, which guarantees that its density is uniform and equal to that of the surrounding environment.

Figure 4: Analysis coordinate system.

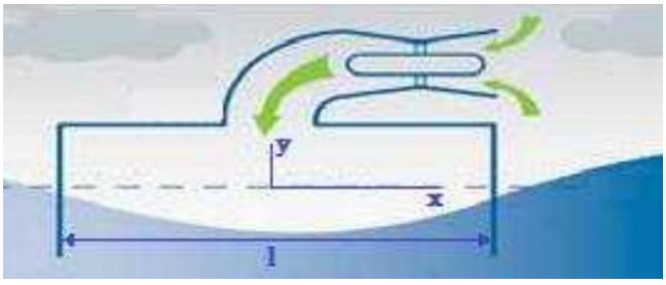

Source: Authors.

The amplitude, wavelength, and velocity terms in the general travelling wave equation is represented below [23].

$$y(x,t) = a\sin\frac{2\pi}{\lambda}(x - ct) \tag{1}$$

Where y is the moving water particles' vertical displacement. The wave height H is twice the amplitude (H =2a), k is the wave number ($k = \frac{2\pi}{\lambda}$), c is wave speed (c = $\frac{\omega}{k}$), and ω is radiant frequency.

$$y(x,t) = \frac{H}{2}\sin(kx - \omega t) \tag{2}$$

The entire volume of the chamber Vc without the volume taken up by the water V_w(t) is the volume of air at any given time V(t):

$$V(t) = V_c - V_w(t) = V_c - \iint y(x,t)dA \tag{3}$$

$$V(t) = V_c - w\int_{-\frac{l}{2}}^{\frac{l}{2}} y(x,t)dx = V_c + \frac{wH}{2k}\left[\cos\left(\frac{kl}{2} - \omega t\right) - \cos\left(\frac{kl}{2} + \omega t\right)\right] \tag{4}$$

$$V(t) = V_c + \frac{wH}{k}\sin\frac{kl}{2}\sin\omega t \tag{5}$$

For the control volume (CV) with mass m_{CV}, the continuity equation for an air chamber can be written as:

$$\dot{m}_{\text{in}} - \dot{m}_{\text{out}} = \frac{dm_{CV}}{dt} \tag{6}$$

where the indices (in) and (out) represent the entering and exiting flow, respectively, and dot (.) signifies the time derivative. Assuming an incompressible fluid flow, $\dot{V}_a(t)$ is the air volume rate through the turbine and t represent the time in seconds.

$$\dot{V}_a(t) = \frac{dV(t)}{dt} = \frac{wH\omega}{k}\sin\frac{kl}{2}\cos\omega t = wHc\sin\frac{kl}{2}\cos\omega t \tag{7}$$

The turbine turns the kinetic energy of moving air into mechanical rotational power $\dot{E}_t$ by extracting it from the air's kinetic energy at speed v and mass flow rate $\dot{m}_a$:

$$\dot{E}_t = \frac{1}{2}\frac{16}{27}\dot{m}_a v^2 = \frac{8\varrho}{27A_c^2}\dot{V}_a(t)^3 \tag{8}$$

$$\dot{E}_t = \frac{8\varrho}{27A_c^2}w^3H^3c^3\sin^3\left(\frac{kl}{2}\right)\cos^3(\omega t) \tag{9}$$

where ϱ is the density of air and (Ac) is the cross section are of the turbine. The total delivered mechanical power (Et) during one cycle or period T of the incident wave can be written as:

$$E_t = 4\int_0^{T/4}\dot{E}_t dt = \frac{32\varrho}{27A_c^2}w^3H^3c^3\sin^3(\frac{kl}{2})[\frac{1}{\omega}\sin\frac{\omega T}{4} - \frac{1}{3\omega}\sin^3\frac{\omega T}{4}] \tag{10}$$

where the integral is determined in a quarter of a period rather than a whole period. The surface water below the mean surface line thereby causes the negative sign to appear for the air volume in figure four. Since ωT = 2π, the periodic energy Et and the average power Pa can be calculated as follows:

$$E_t = \frac{32}{81\pi A_c^2}\varrho T w^3H^3c^3\sin^3(\frac{kl}{2}) \tag{11}$$

$$P_a = \frac{32\varrho}{81\pi A_c^2T^2}w^3H^3\lambda^3\sin^3(\frac{\pi l}{\lambda}) \tag{12}$$

If the depth of the seawater in which it travels is taken to be mathematically infinite, it is simple to estimate the strength of an ocean wave that is perfectly sinusoidal and flowing in a single direction. In practical terms, it is assumed that the depth exceeds half of a wavelength. Under these conditions, it can be seen that the mean power transmitted for the wave front's width in the direction of propagation is stated as follows. [24]:

$$P_w = \frac{\rho g^2}{32\pi}H^2Tw \tag{13}$$

where ρ is the density of sea water. and g is the acceleration of gravity. The more extensive equation for the transfer of wave power is [25]:

$$P_w = Encw \tag{14}$$

$$n = \frac{1}{2}(1 + \frac{2kh}{\sinh 2kh}) \tag{15}$$

and E is the time-averaged, wave-induced energy (potential E_p plus kinetic E_k) per unit horizontal area:

$$E = E_k + E_p = \frac{1}{2}\rho g^2 a \tag{16}$$

The efficiency η of the OWC device is simply determined by:

$$\eta = \frac{P_a}{P_w} = 0.131 \frac{\varrho w^2 H c^3}{\rho A_c^2 T} \sin^3\left(\frac{kl}{2}\right) \quad (17)$$

$$\eta = 0.131 \frac{\varrho w^2 H \lambda^3}{\rho A_c^2 T^4} \sin^3\left(\frac{\pi l}{\lambda}\right) \quad (18)$$

3. OWC simulation.

The most effective way to generate numerical solutions is through CFD modelling by means of ANSYS FLUENT to study the air velocity entering the turbine. The system of the OWC is computationally analyzed to examine the air flow properties that directly affects the turbine's output power using a Volume of Fluid model (VOF) in ANSYS FLUENT. The contact between the air and water phases is established using the VOF technique. The multiphase of two fluids is computed by using the piecewise-linear method. To investigate the air properties within the air chamber of an OWC system. An illustration of an OWC wave energy converting system is developed in this research. The walls, together with all input and output parameters, are specified during this stage to create the boundary conditions. The wave regime is shallow/intermediate, and the wave theory is Stokes of fifth order. Wave length (L) is 11 meters, wave height (H) is 1.3 meters, and liquid depth (d) is 6 meters. Figure five shows the fine mesh and the main geometrical elements.

Figure 5: The geometric dimensions and the fine mesh.

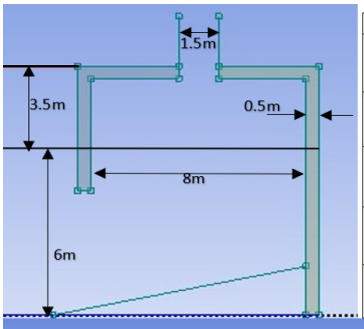

Model dimensions	
Hole diameter	1 m
Free surface elevation	3.5 m
Still water depth	6 m
Chamber length	8 m
Skirt thickness	0.5 m

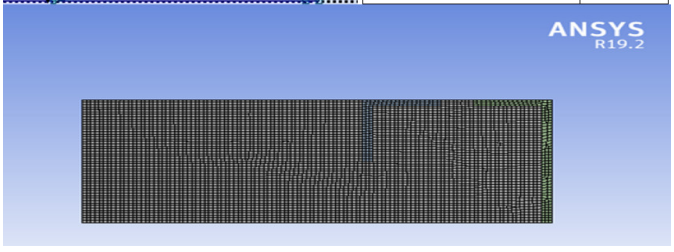

Source: Authors.

The air velocity results of the OWC simulation show a maximum velocity of 7 m/s. Experimental outputs from KORDI's physical modelling test (Hong et al., 2007) indicated that the simulation numerical results were validated as well as approximately equivalent to the experimental results [2]. The air flow velocity is the most critical part of this study since the air characteristics will be applied in the CRSWT simulation. The objective of this study is to simulate the turbine individually to investigate its performance and optimize its output power. Figure six shows the water volume fraction and time of air flow rate.

Figure 6: The water volume fraction and the rate of air flow.

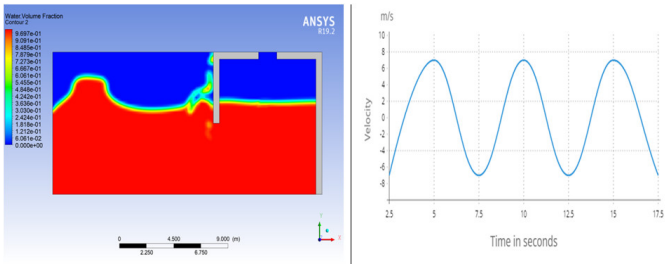

Source: Authors.

4. Methodology.

The air turbine design is critical to maximize the power output and overall efficiency of OWC device. The primary objective of the current study is to focus on the impact of CRWT Savonius S-type rotor performance by using computation fluid dynamic (CFD) analysis. When analyzing the performance of a air turbine, the aerodynamic quantities such as tip-speed ratio (TSR), torque, and power are primarily computed.

The experimental power out P_{ex} is shown in the following equation:

$$P_{ex} = \omega T_m \quad (19)$$

where ω and T_m are respectively the rotor speed and the mechanical torque. The theoretical power P_T and theoretical torque T_T in the wind:

$$P_T = \frac{1}{2}\rho A V^3 \quad (20)$$

$$T_T = \frac{1}{2}\varrho\, V A^2 R \quad (21)$$

where ϱ is the air density, A represents the estimated area on the rotor, V represents air velocity and R is the blade radius.

4.1. Model geometry.

Figure seven shows the layout of S-type CRSWT, and table one represents the geometric specifications of S-type CRSWT.

Table 1: Turbine dimension.

Specification	Values
Blades type	S type
Blades amount	3
Diameter of the blade	60 cm
Blade Height	1.2 cm
The thickness	0.5 cm

Source: Authors.

Figure 7: S-type CRSWT layout.

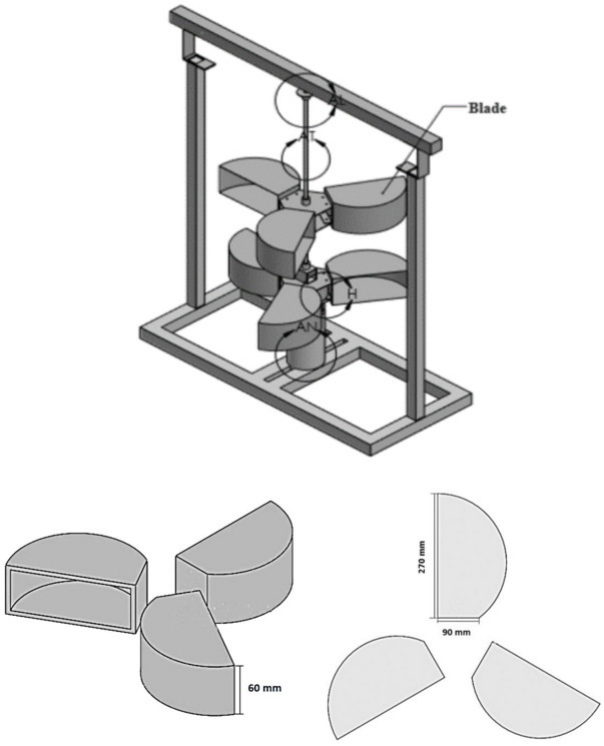

Source: Authors.

4.2. CFD simulation.

The simulation only included consideration of the blades, as seen in Figure seven. As indicated in Figure eight, the computational domain is divided in to two separate zones: moving and stable zones. The fixed zone is the simulation's calculating region, and the rotating circular zone belongs to the moving domain where the two counter-rotating rotors turn. Furthermore, the moving zones have been separated into two subzones. Zone for every rotor (the higher rotor and lower rotor), because they spin in opposite orientations.

Figure 8: The simulated model domain.

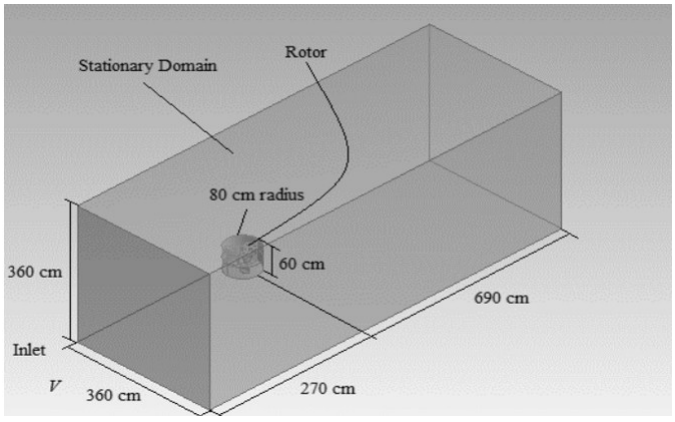

Source: Authors.

At the model's inlet and outflow areas, uniform velocity inlet and pressure outlet boundary conditions are utilized. Furthermore, the bottom, top, and lateral walls are designated as non-slip wall boundary conditions. Between the top and bottom domains, as well as between the rotating and fixed zones, nonconformal interface boundary constraints are applied. As illustrated in Figure nine, the present model is subjected to structured mesh, with a fine mesh at the blade walls. The maximum skewness is less than 0.85.

Figure 9: Fine mesh for the blade.

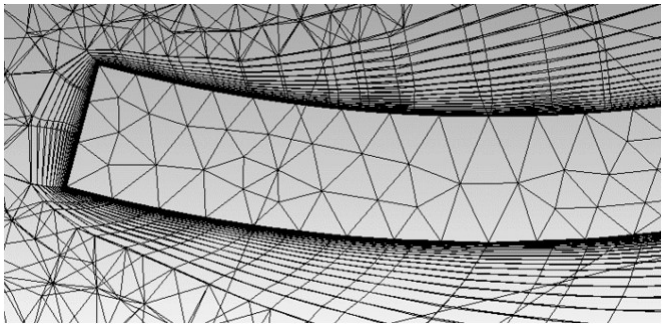

Source: Authors.

4.3. Solution setup.

The governing flow equations are resolved by the flow solver, while ANSYS FLUENT runs the input data. In the current design, the built-in application FLUENT 19.1 in ANSYS software is used to model and simulate fluid flow. The fluid flow is utilized by applying the incompressible unsteady Reynolds-averaged Navier-Stokes (RANS) equations. The k-omega shear stress transfer (SST) model was used to simulate turbulent viscosity. As the solution approach for the simulation process, the pressure-velocity coupling algorithm was used. Different air speed ranges from 2m/s to 9 m/s are applied in this study.

5. Verification and validation

The identical sequence of wind velocity measurements that were used to produce outcomes are used in [26], [27]. The present study's findings are comparable to those of earlier experiments with a relative error of roughly 12%, which increases the confidence in the ability of the current simulation settings to forecast the desired outcomes [27]. This boosts confidence in the capability of the present simulation setup to forecast the desired outcomes.

6. Results and discussion

Based on the Savonius S-type rotor and utilizing a computational simulation approach, the results show the achievement of a CRWT. Airflow rates ranging from 2 m/s to 9 m/s were used to evaluate the model. The findings demonstrate how the rotors' output power varies significantly with air velocity. The CRWT model's power output progressively increases with increasing wind speed. The results show that the counter-rotating model performs substantially better than a single-rotor design,

leading to an improvement in turbine performance. Over twice the output power of SRWT is produced by a CRWT system. The highest output power of the CRWT is 18 W at 9 m/s air velocity, whereas the individual power of the bottom rotor at the same speed is not greater than 3 W. According to the results, the torque of the bottom rotor evaluated individually is equal to 360% of the maximum torque of the CRWT. The produced power capabilities of the current counter-rotating configuration are shown in Figure ten. The results of the modelling and simulation illustrate the practicality and impact of the counter-rotation principle when used with a Savonius VAWT. Testing of the model was done at air flow rates between 2 m/s and 9 m/s. According to reports, the power of the rotors fluctuates greatly with wind speed. The power generated from the CRWT design progressively rises as wind speed rises.

Figure 10: Output power with respect to the airflow velocity.

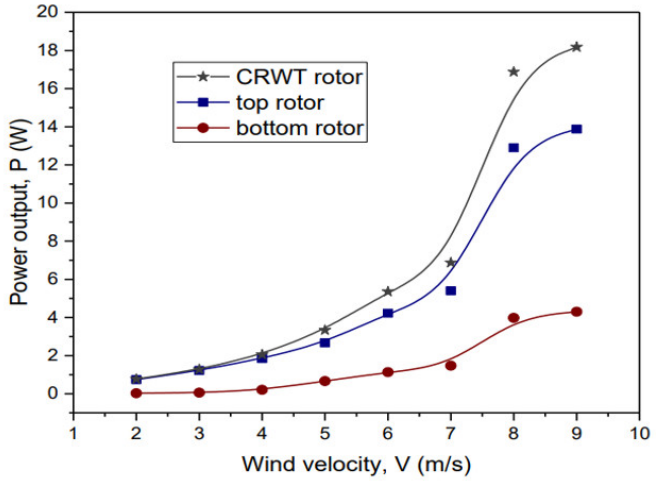

Source: Authors.

The results show that at an air velocity of 2 m/s, the power output reaches a maximum of 1 W in the CRWT design, while at an air speed of 9 m/s, the output power reaches 18 W in the CRWT design and 5 W in the single rotor design. According to Figure ten, the top rotor significantly increased the turbine's power output, which was difficult to achieve with a typical single-rotor Savonius VAWT. Additionally, the top rotor's higher rotational speed resulted in a higher equivalent power output than the bottom rotor. The amount of energy generated by both rotors tends to grow when the top and bottom rotors are measured, and the difference gets greater as the upstream wind speed rises. With low-speed air flow in particular, the performance of this unique design at lower speeds can be advantageous for energy conversion. As illustrated in Figure eleven, the average torque output increases steadily with increasing air velocity for both the upper and lower rotors. Because of the raised rotational speed of the upper rotor, it produces more power than the lower one. therefore, the total generated power of (CRWT) from the two rotors is more than twice as high as that of the single-rotor.

Figure 11: Torque output with respect to airflow velocity.

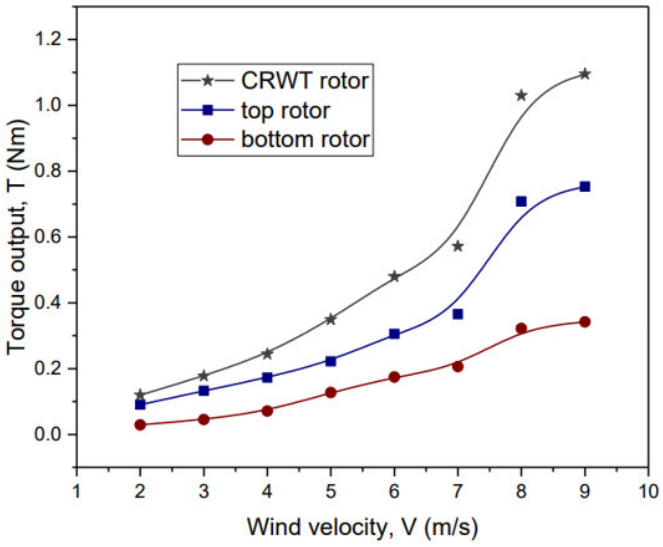

Source: Authors.

Figure twelve displays velocity contours for upstream wind, showing a lower rotor's velocity contour in comparison to the top rotor due to the lower rotational speed of the bottom rotor. The velocity distribution at the blades is more at the tip and less at the center of rotation.

Figure 12: Velocity contours.

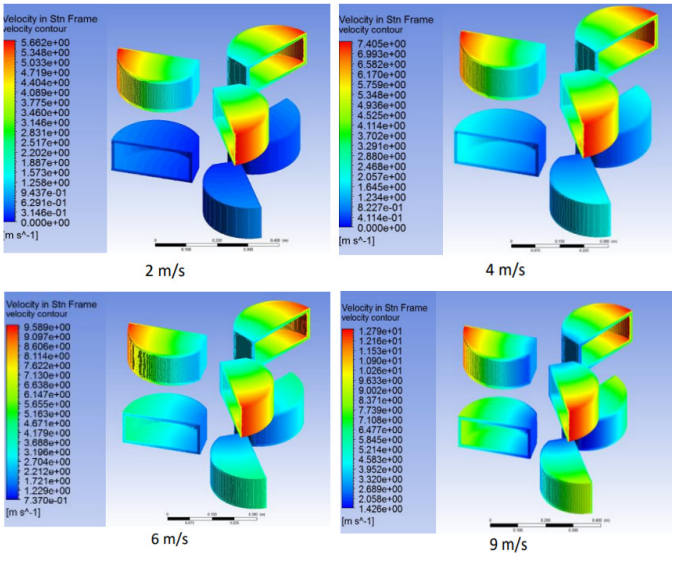

Source: Authors.

Conclusions.

The Oscillating Water Column (OWC) device is an extremely used method for wave energy conversion. This study investigates the efficiency optimization of OWC wave converters by enhancing air turbine performance. The study focuses on the turbine performance as a power take-off in OWC converters. The paper also investigates the modelling and achievement of

a (CRWT) based on the Savonius S-type rotor using a computational simulation approach. The model was evaluated at air flow rates ranging from 2 m/s to 9 m/s. the results show that the output power of the rotors differs greatly according to the air velocity. With increasing wind speed, the CRWT model's power output gradually rises. According to the results, the counter-rotating model exceeds a single-rotor design in terms of performance, which significantly improves turbine performance. The CRWT system generates more than twice the maximum power of an SRWT. The maximum output power for CRWT is 18 W at an air velocity of 9 m/s, while the power of the bottom rotor individually at the same speed doesn't exceed 3 W. The results also show that the maximum torque of the CRWT equals 360% of the torque of the bottom rotor individually.

References.

1. El gohary, M. Morsy and Seddiek, I., (2013). Utilization of alternative marine fuels for gas turbine power plant onboard ship. International Journal of Naval Architecture and Ocean Engineering, 5(1), pp.141-149. https://doi.org-/10.2478/IJNAOE-2013-0115.
2. Elmallah, M., Elgohary, M. M., & Shouman, M. R. (2023, February 27). The Effect of Air Chamber Geometrical Design for Enhancing the Output Power of Oscillating Water Column Wave Energy Converter. Marine Technology Society Journal, 57(1), 122–129. https://doi.org/10.-4031/mtsj.57.1.14.
3. Falcao A. Wave energy utilization: a review of the technologies. Renew Sustain Energy Rev 2010; 14(3):899–918. https://doi.org/10.1016/j.rser.2009.11.003.
4. Cui, Ying & Liu, Zhen. (2014). Effects of Solidity Ratio on Performance of OWC Impulse Turbine. Advances in Mechanical Engineering, 7(1), 121373. https://doi.org/10-.1155/2014/121373.
5. Sameti, M. and Farahi E., (2014). Output Power for an Oscillating Water Column Wave Energy Conversion Device. Oric Pubication.
6. Mitulet, Lucia-Andreea, Gabriela Oprina, Rares-Andrei Chihaia, Sergiu Nicolaie, Adrian Nedelcu, and Mihail Popescu. "Wind tunnel testing for a new experimental model of counter-rotating wind turbine." Procedia Engineering 100 (2015): 1141-1149. https://doi.org/10.1016/-j.proeng.2015.01.477.
7. Shouman, M. R., & Helal, M. M. (2023, July). Numerical investigation of improvement of counter rotating Savonius turbines performance with curtaining and fin addition on blade. Alexandria Engineering Journal, 75, 233–242. https://doi.org/10.1016/j.aej.2023.05.002.
8. D.H. Didane, N. Rosly, M.F. Zulkafli, S.S. Shamsudin, Performance evaluation of a novel vertical axis wind turbine with coaxial contra-rotating concept, Renew. Energy 115 (2018) (2018) 353–361, https://doi.org/10.1016/-j.renene.2017.08.070.
9. D.H. Didane, N. Rosly, M.F. Zulkafli, S.S. Shamsudin, Numerical investigation of a novel contra-rotating vertical axis wind turbine, Sustain. Energy Technol. Assess. 31 (2019), https://doi.org/10.1016/j.seta.2018.11.006.
10. Didane, D. H., Maksud, S. M., Zulkafli, M. F., Rosly, N., Shamsudin, S. S., & Khalid, A. (2019). Experimental Study on the Performance of a Savonius-Darrius Counter-Rotating Vertical Axis Wind Turbine. IOP Conference Series: Earth and Environmental Science, 268(1), 012060. https://doi.org/10.1088/1755-1315/268/1/012060.
11. D.H. Didane, S.M. Maksud, M.F. Zulkafli, N. Rosly, S.S. Shamsudin, A. Khalid, Performance investigation of a small Savonius-Darrius counter-rotating vertical-axis wind turbine, Int. J. Energy Res. (2019), https://doi.org/10.1002-/er.4874.
12. Fujisawa N. (1996). Velocity measurements and numerical calculations of flow fields in and around Savonius rotors, Journal of Wind Engineering and Industrial Aerodynamics (59) 39–50.
13. Fujisawa N. (1992). On the torque mechanism of Savonius rotors, Journal of Wind Engineering and Industrial Aerodynamics (40) 277–292.
14. Fujisawa N and Gotoh F. (1994). Experimental study on the aerodynamic performance of a Savonius rotor, Journal of Solar Energy Engineering, Transactions of the ASME (116) 148–152.
15. Fujisawa N and Gotoh F. (1992). Pressure measurements and flow visualization study of a Savonius rotor, Journal of Wind Engineering and Industrial Aerodynamics (39) 51–60.
16. Fujisawa N and Taguchi Y. (1993). Visualization and image processing of the flow in and around a Savonius rotor, Journal of Flow Visualization and Image Processing 1 (337–346).
17. Fujisawa N and Shirai H. (1987). Experimental investigation on the unsteady flow field around a Savonius rotor at the maximum power performance, Wind Engineering 11 (4) 195–206.
18. Fujisawa N and Gotoh F. (1992). Visualization study of the flow in and around a Savonius rotor, Experiments in Fluids (12) 407–412.
19. Aldoss T K and Kotb M A. (1991). Aerodynamic loads on a stationary Savonius rotor, JSME International Journal Series II 34 (1) 52–55.
20. Aldoss T K and Kotb M A. (1988). Theoretical calculations of the flow field around a Savonius rotor, Wind Engineering 12 (3) 194–203.
21. Fernando M S U K and Modi V J. (1989). A numerical analysis of the unsteady flow past a Savonius wind turbine, Journal of Wind Engineering and Industrial Aerodynamics (32) 303–327.
22. Ishimatsu K, Kage K and Okubayashi T. (2002). Numerical study for the flow fields and performances of Savonius-type and Bach-type rotors, in: The 10th International Symposium on Flow Visualization, Kyoto, Japan, pp. 1–7.

23. Twidell, J., & Weir, T. (2012). Renewable energy resources ED2. Taylor & Francis.
24. Clément, A., McCullen, P., Falcão, A., Fiorentino, A., Gardner, F., Hammarlund, K., Lemonis, G., Lewis, T., Nielsen, K., Petroncini, S., Pontes, M. T., Schild, P., Sjöström, B. O., Sørensen, H. C., & Thorpe, T. (2002, October). Wave energy in Europe: current status and perspectives. Renewable and Sustainable Energy Reviews, 6(5), 405–431. https://doi.org/10.1016/s1364-0321(02)00009-6.
25. Bridges, T. J. (2008, October). WAVES IN OCEANIC AND COASTAL WATERS, by Leo H. Holthuijsen, Cambridge University Press, 2007. ISBN 978-0521860284. 387 pp. Quarterly Journal of the Royal Meteorological Society, 134(636), 1947–1948. https://doi.org/10.1002/-qj.324.
26. _L.-A. Mitulet, G. Oprina, R.-A. Chihaia, S. Nicolaie, A. Nedelcu, M. Popescu, Wind tunnel testing for a new experimental model of counter-rotating wind turbine, Procedia Eng. 100 (2015) 1141–1149, https://doi.org/10.10-16/j. proeng.2015.01.477.
27. Didane, D. H., Saipul Anuar, M. A. Z., Mohideen Batcha, M. F., Abdullah, K., Mohd Ali, M. F., & Mohammed, A. N. (2020, April 20). Simulation Study on the Performance of a Counter-rotating Savonius Vertical Axis Wind Turbine. CFD Letters, 12(4), 1–11. https://doi.org/10.37-934/cfdl.12.4.111.

Nomenclatures	
Ac	turbine cross sectional area, m^2
C	Wave speed, ms^{-1}
Ek	Kinetic energy, J
Ep	Potential energy, J
$\dot{E}_t$	Mechanical rotational power, W
Et	The total delivered mechanical power, W
g	Gravity acceleration, m/s^2
H	Wave height, m
k	Wave number, m^{-1}
ma	Mass flow rate, kg/s
mCV	Mass of control volume, kg
Pa	The average power, W
Pex	Experimental power out, W
Pt	Theoretical power, W
R	Radius of the plate, m
Tm	Mechanical torque, N-m
Tt	Theoretical torque, N-m
V	The velocity of the air, m/s
Vc	Total chamber volume, m^3
Vw(t)	Volume occupied by the water, m^3

Greek Symbols	
η	The efficiency of the OWC device, %
λ	Wavelength, m
ρ	Sea water density, kg/m^3
ϱ	The air density, kg/m3
ω	Radiant frequency, rad/s

Abbreviations	
OWC	Oscillating Water Column
SRWT	Single-rotor wind turbine
VAWT	Vertical axis wind turbine
TSR	Tip-speed ratio
CFD	Computation fluid dynamic
VOF	Volume of fluid